Journal of Thermal Analysis and Calorimetry, Vol. 90 (2007) 3, 747–753

DEHYDROXYLATION KINETIC AND EXFOLIATION OF LARGE MUSCOVITE FLAKES

*F. Gridi-Bennadji and P. Blanchart**

GEMH, Ecole Nationale Supérieure de Céramique Industrielle, Limoges, France

The thermal transformations of muscovite flakes are a key point in many applications because besides dehydroxylation a significant exfoliation process occurs. Dehydroxylation kinetic is experimented by isothermal TG analyses in the 700–850°C temperature range and described with the Avrami theory. Hydroxyl condensation predominates at the onset of the process, but water diffusion is the most important process when the transformed fraction is high. The progressive transition between the two transformation stages contrast with the more accentuated transition for a ground muscovite. The activation energy varies weakly (190–214 kJ mol^{-1}) in the whole transformation process that supports the co-existence of hydroxyl condensation and diffusion phenomena. Dehydroxylation kinetic increases strongly with temperature and decreases with the reaction advancement. Exfoliation is correlated with dehydroxylation kinetic and occurs in a narrow transformation and temperature ranges. An in-situ combination process of hydroxyls occurs and water vapor favors the layer expansion.

Keywords: *dehydroxylation, exfoliation, flakes, muscovite*

Introduction

In the temperature interval for dehydroxylation, muscovite presents very specific DTA and TG curves (Fig. 1), where no well-distinct events can be distinguished. The mass loss at 150°C due to physically adsorbed water attains 0.46 mass%. At 980°C a total of 4.7 mass% is removed, but the most part of hydroxyls is removed below 850°C. The wide temperature interval for dehydroxylation is related to the large distribution of hydroxyl thermal response and a non-homogeneous process should be considered.

Kinetic of dehydroxylation of various micas was investigated 20 years ago by thermal analysis and related to structural characteristics of minerals by I.R. spectroscopy [1]. Recently, the water removal from muscovite was described as a dehydration mechanism, analyzed by the third law method [2]. This approach strongly support the existence of a dissociative evaporation mechanism, but the narrow temperature interval used (778–828°C; 1 bar) and the simple dehydration reaction which is considered, do not reflect the complex relationship between hydroxyl removal and structural transformations in mica layers.

Structural characteristics of well-crystallized 2M1 muscovite [3] are reported in JCPDS files (82-0576). During heating, muscovite structure changes progressively and different structural arrangements were described by Guggenheim [4] (650°C) and Udagawa [5] (900°C). In general, dehydroxylation changes the orientation and mutual positions of tetrahedrons in silicate layers, but at low distance a local order is maintained. Particularly, alumina unit pairs and silica tetrahedron maintain preferential alignments [6–8]. Simultaneously to water departure, dehydroxylation is associated with a significant exfoliation process, that is the expansion of layer distance under the water vapor pressure [9].

TG in isothermal mode at various temperatures, time or atmosphere [4, 5, 10] was used to separate the respective contributions to the mass loss, as physically adsorbed water and structural OH groups. A slow dehydroxylation kinetic is always evidenced, which last up to 2.5 months at 650°C [11]. Such long duration evidences the occurrence of slow processes as water diffusion along layers.

The particle size of muscovite also influences the dehydroxylation process. After different grinding times, DTA and TG curves of Klein [12], Vladimir [13], Lapides [1] and Mackenzie [14] evidenced the occurrence of physically adsorbed water on fine particles surfaces. For finely ground muscovites, dehydroxylation occurs at lower temperature, in a narrow temperature range. Since the occurrence of nucleation and diffusion mechanisms are generally assumed, their respective role in the whole process is changed with particle size. More recently, Pérez-Rodríguez [15] studied the grinding and amorphization processes against the duration of a powerful ultrasound treatment. It increases the specific surface area and reduces significantly the dehydroxylation

* Author for correspondence: p_blanchart@ensci.fr

1388–6150/$20.00

Akadémiai Kiadó, Budapest, Hungary
Springer, Dordrecht, The Netherlands

temperature on DTA and TG curves. Besides, the removal of bulk OH groups can be clearly distinguished from that of the edge OH groups.

Possible successive dehydroxylation stages were distinguished by Gaines and Vedder [16], Kristóf *et al.* [17], and Vassanyi and Szabó [18]. In general, 2 stages are evidenced and the former is the H_2O molecule formation from adjacent OH groups. It is a local reaction, which is followed by water diffusion through the structure and along layers. Mazucatto [19] also proposed a similar description from X-ray patterns of materials in a large temperature range. Nucleation of the dehydroxylated phase is followed by the growing of a high temperature muscovite phase where most of Al ions are five-fold coordinated. Three successive stages can be distinguished when time and temperature increase: – the condensation of adjacent hydroxyls; - unidirectional H_2O diffusion through channels of tetrahedral layers; – bi-directional diffusion of H_2O along interlayer planes. The interpretation of data indicates the predominant role of a unidirectional diffusion mechanism and an activation energy of E_a=250.8 kJ mol^{-1} was reported. This high value in comparison to that of illite (E_a=109 kJ mol^{-1}) reported from Filopovic-Petrovic [20] suggests that it is mostly related to nucleation mechanisms. From other studies on various mica minerals containing iron, Lapides [21] obtained E_1=85 kJ mol^{-1} for the nucleation stage and E_2=380 kJ mol^{-1} for the diffusion stage.

The occurrence of possible mechanism involved in the reaction process can be questioned with the Avrami *n* parameter, which is directly related to the kinetic expression to be used. Particularly, Mazucatto [19] reported a low *n* value (0.29) when the reaction rate is governed by unidirectional diffusion of water. But in the case of a step-by-step reaction process, *n* should change with time and temperature.

The present work is devoted to muscovite dehydroxylation. Experiments are focused on the behavior of large flakes in view to study mechanism involved in dehydroxylation in relation to the exfoliation process. Data from muscovite flakes are compared to those from a fine powder, to identify the mechanisms involved. The dehydroxylation process was followed by TG and DTA in isothermal and dynamic conditions, between 700 and 850°C. In the same temperature and time ranges, the expansion of layers is observed by dilatometry. An interpretation of the reaction rate during flake dehydroxylation is proposed in relation to the extend of the exfoliation process.

Experimental

Muscovite flakes are from Bihar (India) [22]. The chemical and mineralogical compositions are very close to ideal compositions of muscovite. Structural characteristics were found to be very similar to tabulated data in JCPDS files and the structural formula is:

$$(K_{0.93}Na_{0.11})(Al_{1.84}Fe_{0.09}Mg_{0.02}Ti_{0.02})(Si_{3.12}Al_{0.88})O_{10}(OH)_2$$

The quasi-ideal composition ensures that thermal transformations will be very similar to that of an ideal mineral. Dehydroxylation occurs with the reaction:

Muscovite (>550°C)$\rightarrow H_2O+(K_{0.93}Na_{0.11})(Al_{1.84}Fe_{0.09}Mg_{0.02}Ti_{0.02})(Si_{3.12}A1_{0.88})O_{11}$ with a theoretical mass loss of 4.42 mass%. The slightly larger mass loss in Fig. 1 is due to adsorbed water on surfaces (~1 mass%).

Differential scanning calorimetries were performed using a Setsys 2400 apparatus (Setaram) equipped with a DTA-1500 head system. For kinetic interpretations, the instrument was used in the temperature-scanning mode and all experiments were performed from room temperature to 1100°C using six different heating rates (1, 3, 5, 8, 10 and 20°C min^{-1}). Experiment were carried out with 100 mg of powder under ambient atmospheric pressure and a pure alumina powder heated at 1500°C serves as a reference material, but in adequate quantity to reduce the calorimeter imbalance. A typical DTA curve (10°C min^{-1} heating rate) is presented in Fig. 1, which evidences the wide temperature range and the flattened peak shape of dehydroxylation above 330°C.

Kinetic methods, as Kissinger's one, have been extensively used with clay minerals for the interpretation of endothermal and exothermal phenomena in DTA curves, but baseline instability and drift or uncertainty of peak limits interfere with the measurements. The common feature of kinetic methods is the determination of peak temperature *vs*. the scan rate of

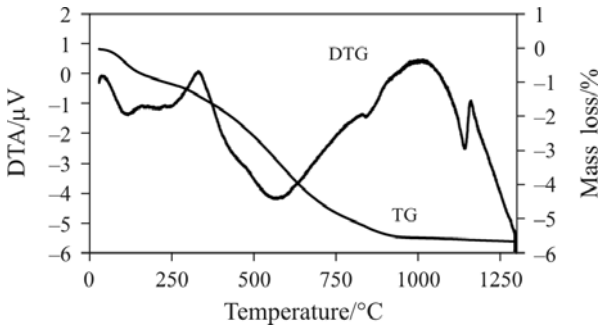

Fig. 1 DTA and TG curves *vs*. temperature at 10°C min^{-1} heating rate for muscovite powder

DTA scans. For the interpretation of data, specific mathematical treatments must be considered, but with some assumptions for calculations [23].

With muscovite powder the DTA peak temperature (Fig. 1) and the fraction of transformed material cannot be accurately determined. Instead of DTA, we used isothermal thermogravimetry (TG) for the characterization of muscovite. Measurements were carried out with a Linseis (L81) TG apparatus, equipped with a large crucible containing stacked layers of muscovite (4×4 mm, 200 mg). Thermal cycles were performed under flowing air with a rapid increase in temperature (50°C min^{-1}), followed by an isothermal stage (±1°C) in the 700–850°C temperature range. The duration of the isothermal stage was 10 to 100 h, to achieve a complete dehydroxylation (4.42 mass%). Curves of dehydroxylated fractions *vs.* temperature are plotted against time in Fig. 2.

The exfoliation process was characterized by dilatometry *vs*. temperature (Misura-System). The thickness of small flakes (4·4·0.1 mm) was measured by image analysis during controlled thermal cycles under flowing air. This technique ensures that no mechanical constraint of any kind is applied to flakes. Two different thermal cycles were used: a temperature ramp at 10°C min^{-1} followed by a temperature stage of 3 h; an isothermal cycle similar to that used for TG measurements. The later experiments was used to characterize the extend of exfoliation *vs*. the transformed fraction of muscovite.

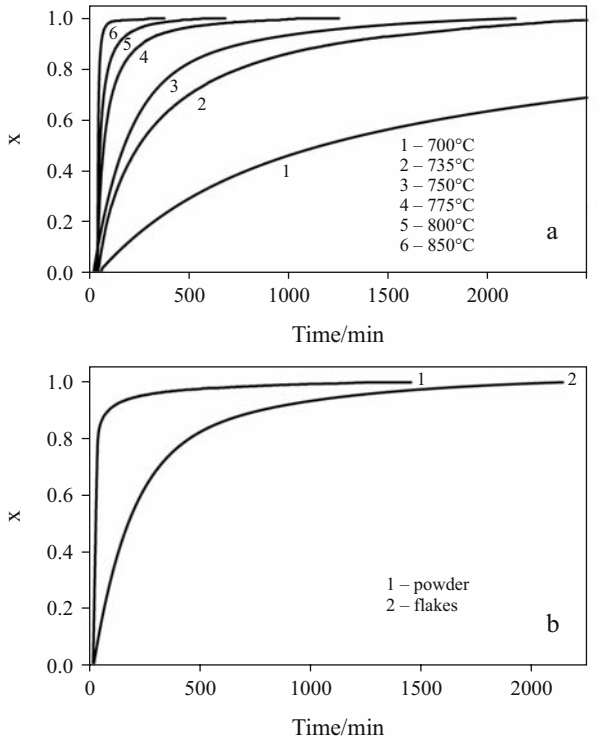

Fig. 2 a – transformed fraction (x) of muscovite flakes *vs*. time in the 700–850°C temperature range; b – muscovite flake behavior in comparison to that of muscovite powder during the same isothermal treatment at 750°C

Results

The Jonhson–Mehl–Avrami (JMA) theory is a representation of the transformed fraction x *vs.* time t, during a phase transformation in isothermal condition.

$$x = 1 - \exp[-(kt)^n] \quad (1)$$

where n is the Avrami exponent related to the mechanism involved in the reaction. The reaction rate k is temperature dependent and expressed by an Arrhenius-type equation:

$$k = k_0 \exp\left(-\frac{E}{RT}\right) \quad (2)$$

where T is the temperature and R the gas constant. k_0 and E are the frequency factor and the apparent activation energy for the reaction, respectively.

For muscovite flakes at 700, 735, 750, 775, 800 and 850°C, the x transformed fraction is plotted in Fig. 2a. It is seen that time to achieve the complete dehydroxylation is highly temperature dependent. In Fig. 2b, the behavior of muscovite flakes is compared to that of muscovite powder during the same isothermal treatment at 750°C. For the ground muscovite, time to attain the complete dehydroxylation is shortened and two transformation stages are clearly distinguished.

The logarithm form of Eq. (1) gives the commonly used expression:

$$\ln[1 - \ln(1-x)] = n \ln k + n \ln t \quad (3)$$

with isothermal experiments at T, Eq. (3) is used to obtain n and k.

Using powder and flakes, experimental representation of Eq. (3) points to the existence of possible succes-

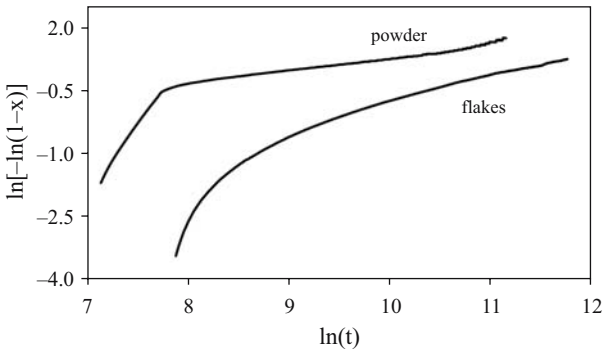

Fig. 3 ln(–ln(1–x)) *vs.* ln(t) at 750°C for muscovite flakes and powder

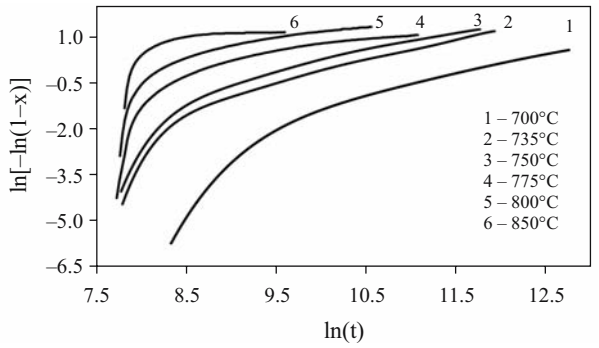

Fig. 4 ln(–ln(1–*x*)) *vs.* ln(*t*) in the 700–850°C temperature range for muscovite flakes

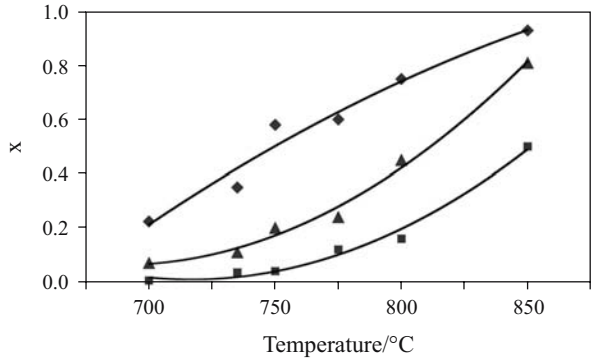

Fig. 5 *x* limiting values for the initial, transitional and final dehydroxylation stages

sive stages during the whole dehydroxylation process (Fig. 3). For muscovite powder, 2 stages with a quasi-linear variation are clearly distinguished. The transition point corresponds to a high value of *x* (~0.8). In the case of flakes (Figs 3 and 4), the existence of 3 successive stages can be assumed [19]. In Table 1, *n* and *k* are calculated for the initial, transitional and final dehydroxylation stages. *x* limiting values between stages, *vs.* temperature, are plotted in Fig. 5.

k at different temperatures (Table 1) can be used with Eq. (2) to calculate the Arrhenius parameters k_0 and *E*. Figure 6 evidences the quasi-linear variation of reaction rates *k vs.* 1/*T*. Calculated activation energies from line slope are reported in Table 2 for 7 values of *x*.

Table 1 Calculated *n* and *k* values for the initial, transitional and final dehydroxylation stages and *x* limiting values between stages

		n	$k_0/10^{-5}$ s^{-1}	R_2
700°C	0.00<*x*<0.05	3.40	4.82	0.99
	0.05<*x*<0.23	1.41	1.71	0.99
	0.23<*x*<0.85	0.64	0.73	0.99
735°C	0.00<*x*<0.12	3.58	14.56	0.98
	0.12<*x*<0.28	1.49	6.87	0.99
	0.28<*x*<1.00	0.68	3.81	0.99
750°C	0.00<*x*<0.20	3.61	16.05	0.97
	0.20<*x*<0.45	1.22	7.15	0.98
	0.45<*x*<1.00	0.59	6.76	0.99
775°C	0.00<*x*<0.24	4.82	25.30	0.98
	0.24<*x*<0.60	1.21	15.24	0.97
	0.60<*x*<1.00	0.39	21.12	0.94
800°C	0.00<*x*<0.45	4.93	29.96	0.98
	0.45<*x*<0.75	1.33	25.67	0.99
	0.75<*x*<1.00	0.41	73.58	0.97
850°C	0.50<*x*<0.80	3.64	37.01	0.97
	0.80<*x*<0.93	1.00	57.09	0.97
	0.93<*x*<1.00	0.35	348.12	0.97

With flakes, limits of successive dehydroxylation stages in Fig. 4 cannot be clearly determined. From isotherms of Fig. 2, it is possible to calculate reaction time constants of possible mechanisms by fitting analytical expressions to the decay of d*x*/d*t* with time. By assuming the existence of 2 or 3 transformation mechanisms, we consider the following exponential analysis:

$$\frac{dx}{dt} = \sum_i A_i \exp\left(\frac{-t}{\tau_i}\right) \quad (4)$$

where *i*=2..3 and $\tau_i = 1/k_i$.

Using only the first 2 terms of Eq. (4), we obtain a good approximation of data (Fig. 2) and significant values of τ_i can be calculated. Arrhenius plots of time constants at various temperatures yield activation energy for each transformation mechanism. In Fig. 7 the temperature dependence of the 2 mechanisms (τ_1 and τ_2) are well described by the Arrhenius equation and values of k_1, k_2, E_1 and E_2 are reported in Table 3.

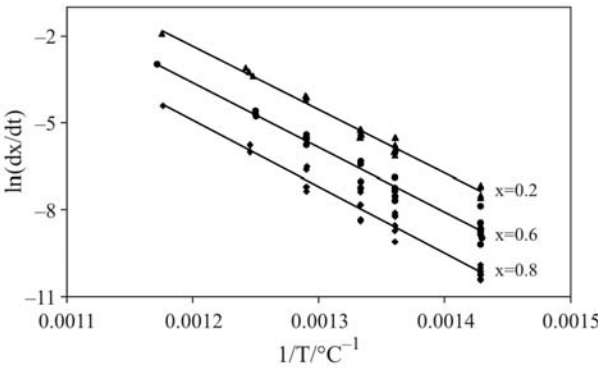

Fig. 6 Arrhenius plots in the 700–850°C temperature range for typical values of *x*

Table 2 Activation energy *E* from Eq. (2) as a function of *x*

x	0.1	0.2	0.3	0.4	0.5	0.6	0.8
E/kJ mol^{-1}	214.42	185.93	183.58	190.55	191.42	185.50	190.44

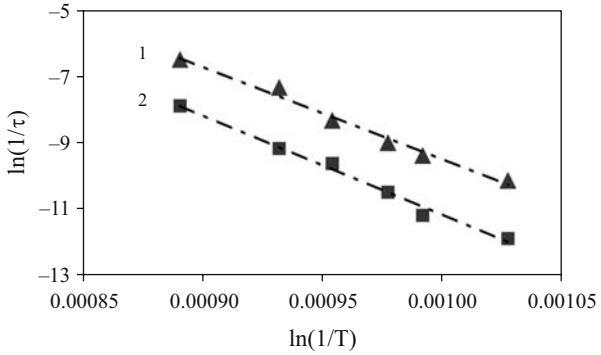

Fig. 7 Arrhenius plots of τ_1 and τ_2 calculated from 2 exponential terms on isothermal dx/dt

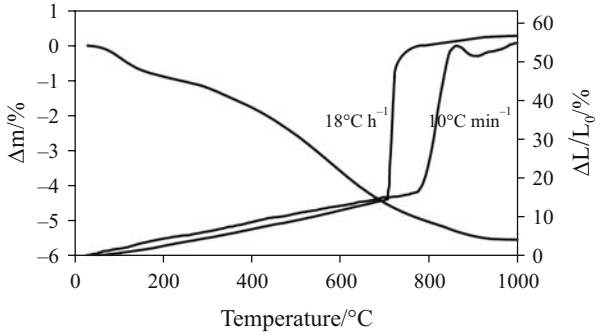

Fig. 8 Dilatation of muscovite flakes *vs*. temperature during a 18°C h^{-1} and a 10°C min^{-1} temperature ramp followed by 3 h at 735°C, in comparison to TG at 10°C min^{-1}

Table 3 Transformation rates and activation energies for k_1, k_2, E_1 and E_2 from 2 exponential terms on isothermal dx/dt

	$k_1/10^{-5}$ s^{-1}	$k_2/10^{-5}$ s^{-1}	R_2
700°C	3.96	0.685	0.99
735°C	8.43	1.38	0.99
750°C	12.46	2.78	0.99
775°C	24.56	6.65	0.99
800°C	66.36	10.46	0.99
850°C	104.65	38.09	0.96
E_1, E_2/kJ mol^{-1}	E_1=233.3	E_2=250.56	0.98

Dilatation experiments during a temperature ramp up to 1000°C are presented in Fig. 8. Exfoliation occurs at 720°C and the layer thickness increases significantly, to attain 1.6 time the initial thickness. During an isothermal experiment at 735°C, we observe that exfoliation starts rapidly after 0.5 h and x=0.12 at 735°C. Exfoliation is achieved after 8.3 h and x=0.65. The thickness variation attains a maximum value of 67% and progressively decreases to 38%.

Discussion

Figures 2a and b point to the existence of 2 main stages separated by a transitional stage during dehydroxylation. For finely ground muscovite, a sharp transition is evidenced in Fig. 2b, but with flakes the dehydroxylation process is progressive.

The interpretation of JMA theory gives large n values (3.4–5.0) for the initial stage and low n values (1.0–1.5) for the transitional and the final stages (Table 1). It means that hydroxyl condensation predominates in a narrow range of x values at the onset of dehydroxylation. Beyond this stage, n values are small in a very large x range. It is typical of a reaction in which the rate limiting step is diffusion along or through layers [16–19], although different interpretations were provided concerning the dimensionality of the diffusion mechanism and the physical interpretation of processes.

Mechanisms occurring during successive stages should be characterized by different activation energy, but activation energies reported in Table 2 does not differ significantly with x, within the error range. The range of E (190–214 kJ mol^{-1} in Table 2) is within the very large variation of reported data by Kodama [24] and recently Mazzucato [25] calculated an average value of 251 kJ mol^{-1}. In general, values differ widely *vs.* experimental conditions (atmosphere or vacuum) or methods (DTA, TG or X-ray).

Table 1 also presents k_0 reaction kinetics during the three stages of Fig. 1. Since the kinetic parameter increases with temperature, the highest kinetic is during the initial dehydroxylation stage. At 800 and 850°C temperatures, the transitional and final stages are within restricted x ranges and non-significant data are obtained. The examination of the isothermal analysis using Eq. (3) leads to the conclusion that activation energy can be obtained accurately but that appreciable error in k_0 can occur when the linear regression is extrapolated to t=0. Nevertheless, below 800°C we found that it is possible to obtain values of k_0 which agree with the wide range of literature data, i.e. 0.38 to $8.0 \cdot 10^{-5}$ s^{-1} at 760–860°C [25] and 1.11 to $214 \cdot 10^{-5}$ s^{-1} at 650–900°C [26].

The application of a single exponent Arrhenius equation (single activation energy) to the process of crystallization can be questioned because the temperature determines the relative contribution of individual processes. Using Eq. (4), the calculated k_1 and k_2 kinetic parameters (Table 3) increase drastically with temperature. These data are comparable to kinetic data in Table 1, although uncertainties relative to data calculated from 800 and 850°C curves exist. The higher k_1 value in comparison to k_2 reflect the significant mass loss at the beginning of dehydroxylation (Fig. 1).

During continuous heating, exfoliation occurs rapidly at low temperature, below 850°C, but the onset of exfoliation depends strongly on the heating rate (Fig. 8). A comparison of the TG and expansion curves (Fig. 8) points to the simultaneous occurrence of accelerating mass loss and exfoliation above 600°C. Expansion attains its maximum value (~60%) at 820°C, during the last stage of the mass loss. The high kinetic of expansion means the early condensation of water molecules and that diffusion is the slower step of the overall reaction.

In isothermal condition at 735°C (Fig. 9), exfoliation occurs rapidly at the beginning of the isothermal stage. The report of x limiting values of Fig. 5 evidences that expansion begins at the end of the initial stage and is achieved at the end of the transitional stage. It means that the high k_0 value during the initial stage triggers the exfoliation process. At higher k_0 values (~0.65), the lower kinetic is accompanied by a significant reduction of expansion.

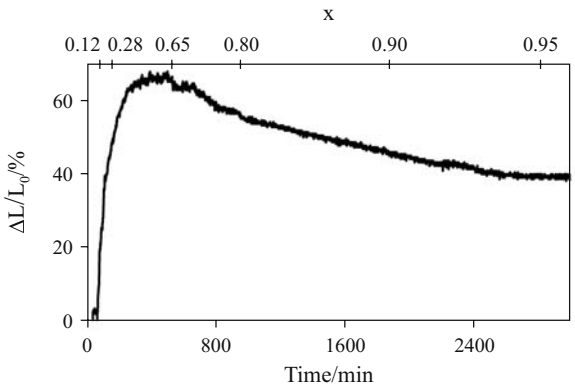

Fig. 9 Dilatation of muscovite flakes during an isothermal experiment at 735°C, for the duration of 55 h

The sequence of reaction involves the dissociation of one hydroxyl group to a free proton and an oxygen ion and the combination of a free proton with a second hydroxyl group to form a water molecule. The combination process occurs either throughout the structure or at a specific region. Proton can diffuse more easily than water molecules, which must migrate towards a gas–solid interface. But with muscovite, an in-situ combination process is more likely to occur and water is formed with essentially the same probability throughout the crystal volume. The significant exfoliation during dehydroxylation evidences the existence of a diffusion-controlled process taking place normal to [001]. The kinetic is then controlled by the escape of water molecules via pores or other defects and induces a high interlayer gas pressure.

Conclusions

TG study of muscovite flakes validates the existence of two main successive stages during dehydroxylation separated by a progressive transitional stage. The two stages are supposed to be related to the condensation of adjacent hydroxyls and to water diffusion through and along layers. The occurrence of these two successive stages is supported by the value of the n Avrami parameter which decreases from ~4 to ~0.4 when the transformed fraction x increases, but activation energies only slightly depend on x. As the variation of n with x contrasts to that with E, during the two stages, it means that hydroxyl condensation predominates in a narrow range of x at the onset of dehydroxylation and that beyond the first stage diffusion becomes the limiting mechanism. Kinetics are strongly enhanced by temperature and decrease with the increase of the x transformed fraction. Water vapor induces a significant exfoliation mechanism of layers during dehydroxylation. Expansion cannot be easily controlled due to its large extent in narrow temperature and transformation ranges.

References

1 I. L. Lapides, J. Thermal Anal., 42 (1994) 197.
2 B. V. L'vov and V. L. Ugolkov, J. Therm. Anal. Cal., 82 (2005) 15.
3 J. Liang and F. C. Hawthorne, Can. Mineral., 34 (1996) 115.
4 S. Guggenheim, Y. Chang and A. H. Foster van Gross, Am. Miner., 72 (1987) 537.
5 S. Udagawa, K. Urabe and H. Hasu, Jpn. Assoc. Mineral., Petrol. Econ. Geol., 69 (1974) 381.
6 C. Rodriguez-Navarro, G. Cultrone, A. Sanchez-Navas and E. Sebastian, Am. Miner., 88 (2003) 713.
7 K. J. D. Mackenzie, I. W. M. Brown, C. M. Cardile and R. H. Meinhold, J. Matter Sci., 22 (1987) 2645.
8 G. Lecomte and P. Blanchart, J. Mater Sci., 41 (2006) 4937.
9 R. W. Lawson, Vacuum, 12 (1962) 145.
10 S. G. Barlow and D. A. C. Manning, Br. Ceram. Trans., 98 (1999) 122.
11 J. P. Eberhart, Bull. Soc. Fr. Miner. Crist., 86 (1963) 213.
12 H. H. Klein, W. B. Stern and W. Weber, Schweiz. Miner. Petrogr. Mitt., 62 (1982)145.
13 V. Hanykyr, J. Ederova and J. Srank, Thermochim. Acta, 93 (1985) 633.
14 K. J. D. Mackenzie, I. W. M. Brown, C. M. Cardile and R. H. Meinhold, J. Mater Sci., 22 (1987) 2645.
15 J. L. Pérez-Rodríguez, J. Pascual, F. Franco, M. C. Jiménez de Haro, A. Duran, V. Ramírez del Valle and L. A. Pérez-Maqueda, J. Eur. Ceram. Soc., 26 (2006) 747.
16 G. L. Jr. Gianes and W. Vedder, Nature, 201 (1964) 495.

17 J. Kristóf, I. Vassanyi, E. Nemecz and J. Inczédy, Thermochim. Acta, 93 (1985) 625.
18 I. Vassanyi and A. Szabó, Mater. Sci. Forum, 133–136 (1993) 655.
19 E. Mazzucato, G. Artioli and A. Gualtieri, Mater. Sci. Forum, 278–281 (1998) 424.
20 L. Filopovic-Petrovic, Lj. Kostic-Gvozdenovic, S. Eric-Antonic and S. Despotovic, Interceram, 48 (1999) 42.
21 I. L. Lapides, J. Thermal Anal., 50 (1997) 269.
22 H. H. Klein, W. B. Stern and W. Weber, Schweiz. Miner. Petrogr. Mitter., 62 (1982) 145.
23 E. Brown, Handbook of Thermal Analysis and Calorimetry, Elsevier, Amsterdam 1998.
24 H. Kodama and J. E. Brydon, Trans. Faraday Soc., 64 (1968) 3112.
25 E. Mazzucato, G. Artioli and A. Gualtieri, Phys. Chem. Miner., 26 (1999) 375.
26 E. A. Kalinichenko and A. S. Litovchenko, Phys. Chem. Miner., 24 (1997) 520.

Received: July 26, 2006
Accepted: February 28, 2007
OnlineFirst: June 28, 2007

DOI: 10.1007/s10973-006-7888-4